Christiane Katharina Kuhl, MD
Peter Mielcareck, MD
Sven Klaschik, MD
Claudia Leutner, MD
Eva Wardelmann, MD
Jürgen Gieseke, PhD
Hans H. Schild, MD

Index terms:
Breast neoplasms, 00.31, 00.32
Breast neoplasms, MR, 00.121412, 00.121415, 00.12143, 00.12144
Magnetic resonance (MR), flow studies, 00.12143, 00.12144

Radiology 1999; 211:101–110

Abbreviation:
ROI = region of interest

[1] From the Departments of Radiology (C.K.K., P.M., S.K., C.L., H.H.S.) and Pathology (E.W.), University of Bonn, Sigmund-Freud-Str 25, D-53105 Bonn, Germany, and Philips Medical Systems, Hamburg, Germany (J.G.). From the 1996 RSNA scientific assembly. Received March 2, 1998; revision requested May 5; final revision received August 5; accepted October 7. **Address reprint requests to** C.K.K.

See also the editorial by Orel (pp 5–7) in this issue.

Author contributions:
Guarantor of integrity of entire study, C.K.K.; study concepts and design, C.K.K.; definition of intellectual content, C.K.K.; literature research, S.K.; clinical studies, C.K.K., P.M., S.K., C.L.; data acquisition, C.K.K., P.M., C.L., E.W.; data analysis, C.K.K., P.M., S.K., E.W.; statistical analysis, C.K.K., J.G.; manuscript preparation and editing, C.K.K.; manuscript review, H.H.S.

Dynamic Breast MR Imaging: Are Signal Intensity Time Course Data Useful for Differential Diagnosis of Enhancing Lesions?[1]

PURPOSE: To assess the relevance of the signal intensity time course for the differential diagnosis of enhancing lesions in dynamic magnetic resonance (MR) imaging of the breast.

MATERIALS AND METHODS: Two hundred sixty-six breast lesions were examined with a two-dimensional dynamic MR imaging series and subtraction postprocessing. Time–signal intensity curves of the lesions were obtained and classified according to their shapes as type I, which was steady enhancement; type II, plateau of signal intensity; or type III, washout of signal intensity. Enhancement rates and curve types of benign and malignant lesions were compared.

RESULTS: There were 101 malignant and 165 benign lesions. The distribution of curve types for breast cancers was type I, 8.9%; type II, 33.6%; and type III, 57.4%. The distribution of curve types for benign lesions was type I, 83.0%; type II, 11.5%; and type III, 5.5%. The distributions proved significantly different ($\chi^2 = 139.6$; $P < .001$). The diagnostic indices for signal intensity time course were sensitivity, 91%; specificity, 83%; and diagnostic accuracy, 86%. The diagnostic indices for the enhancement rate were sensitivity, 91%; specificity, 37%; and diagnostic accuracy, 58%.

CONCLUSION: The shape of the time–signal intensity curve is an important criterion in differentiating benign and malignant enhancing lesions in dynamic breast MR imaging. A type III time course is a strong indicator of malignancy and is independent of other criteria.

The differential diagnosis of enhancing lesions in breast magnetic resonance (MR) imaging is a difficult task. With the technical equipment that is currently available, two concepts have evolved in an attempt to improve diagnostic accuracy. First, high-spatial-resolution single-breast MR imaging studies are used to analyze the lesions' morphologic characteristics, including their internal architecture (1–5). Second, fast imaging protocols with high temporal resolution have been suggested for analysis of the lesions' enhancement behavior (6). Unfortunately, for the time being, fast imaging is available only as a single-section technique. Accordingly, this technique does not seem to be suitable for some potentially important clinical applications of breast MR imaging (eg, preoperative local staging to rule out multicentric tumor growth) (1,4,7).

To compromise on the diverging demands of adequate spatial and temporal resolution, a dynamic breast MR imaging method was introduced several years ago (8–12). In this method, both entire breasts are imaged rapidly and repetitively within a given time frame and with limited spatial resolution. With use of dynamic data sets, two different criteria may be used to describe lesion enhancement kinetics. First, behavior of signal intensity in the early phase after the administration of contrast material is evaluated by means of the steepness of the postcontrast signal intensity curve; several descriptors are in use for this criterion: ''curve slope,'' ''early-phase enhancement rate,'' or ''enhancement velocity,''

which are given by the percentage of increase in signal intensity with respect to the signal intensity before the administration of contrast material.

Second, the behavior of signal intensity in the intermediate and late postcontrast periods may be traced to derive diagnostic information. This time course is visualized by placing a region of interest (ROI) on the lesion to plot the time–signal intensity curve. Visual or quantitative evaluation is focused on the shape of the time–signal intensity curve: whether the signal intensity continues to increase after the initial upstroke, whether it is cut off and reaches a plateau, or whether it washes out.

The diagnostic value of the early-phase enhancement rate criterion has been established by the findings of several recent studies (6,8,9,11). However, it is still a matter of debate whether the signal intensity behavior in the intermediate and late postcontrast phases (ie, the shape of the time–signal intensity curve) conveys diagnostically useful information—specifically, with the temporal resolution achievable with a whole-breast dynamic technique—and, accordingly, whether it is worthwhile to sacrifice some spatial information to evaluate kinetic signal intensity time course data.

Thus, the objectives of this study were to clarify the following issues: Is the time course of lesion signal intensity (ie, the shape of the time–signal intensity curve) useful for the differential diagnosis of enhancing lesions? And if so, how accurate is this criterion? How is its diagnostic accuracy compared with that of the early-phase enhancement rate as the established diagnostic criterion of dynamic breast MR imaging? Is the visual classification of the shape of the time–signal intensity curve reliable enough to allow a reproducible classification of enhancement kinetics? How stable is this criterion (ie, how is the interreader variability)?

MATERIALS AND METHODS

Study Design

The study was a prospective trial with a standardized protocol. The protocol was tailored to selectively determine the diagnostic utility of signal intensity time course analysis in dynamic breast MR imaging (ie, to elucidate its specific contribution to the differential diagnosis of enhancing lesions in breast MR imaging). Accordingly, time–signal intensity curves of enhancing lesions were plotted and presented to two radiologists (C.K.K., P.M.) who were blinded to any clinical or mammographic information of the patients. The radiologists were asked to rate the time courses as having a steady, plateau, or washout shape—type I, II, or III, respectively.

The classification of the lesions on the basis of the time course analysis was then compared with both the breast MR imaging diagnosis without time course analysis (ie, based on enhancement rates) and with the lesions' definitive diagnoses. The definitive diagnosis was obtained histologically by means of excisional biopsy or by means of follow-up in the cases that, on the basis of history, clinical, mammographic, ultrasonographic (US), and breast MR imaging findings, were rated to be probably benign (details of the follow-up protocol are described later).

The study design and protocol were reviewed and approved by the authors' institutional review board; all patients gave informed consent to be examined after the nature of the procedure had been fully explained.

Patients and Inclusion Criteria

A total of 230 consecutive patients (mean age, 45.5 years ± 13 [SD]; range, 21–75 years) with 266 contrast material–enhancing lesions were included in the study. The only inclusion criterion was the presence of a suggestively enhancing area in the breast. Suggestive enhancement in this context was defined as early-phase contrast enhancement that was apparent in the first postcontrast image, because this has been associated with malignant tumor growth (11,13–17), or contrast enhancement with suggestive morphology. Lesion morphology was considered suggestive in lesions with ill-defined borders or irregular contours.

Accordingly, we included only cases with contrast enhancement that was rated as suggestive and that gave rise to differential diagnostic considerations. Negative breast MR imaging studies without contrast enhancement or with nonsuggestive contrast enhancement were excluded to give an authentic and accurate evaluation of the differential diagnostic potency of the criteria under investigation.

Definitive lesion classification was obtained by means of excisional biopsy (162 of 266 lesions) or follow-up over at least 2 years (104 of 266 lesions). Follow-up of the presumed benign lesions consisted of clinical, mammographic, and US control studies and breast MR imaging studies. The follow-up period has been maintained for more than 3.5 years in 16 (15%), for more than 3 years in another 47 (45%), and for more than 2 years in the remaining 41 (39%) of 104 lesions; no change of diagnosis occurred during follow-up.

Breast MR Imaging Technique

Breast MR imaging was performed with use of a 1.5-T system (ACS II; Philips Medical Systems, Best, the Netherlands) by using a standard dedicated bilateral breast coil. The imaging protocol consisted of an initial scout view that provided axial, coronal, and sagittal images of the left and the right breast. These scout images were used to exactly localize the spatial distribution of the parenchymal volume in both breasts. The subsequent axial dynamic series was then positioned (and angled if appropriate) to cover the whole parenchyma.

Two-dimensional imaging was performed with 220/4.5 (repetition time msec/echo time msec), a flip angle of 80°, one signal acquired, 21 sections, a 256 × 192 image matrix, and an imaging time of 42 seconds per dynamic image. The section thickness was 4 mm without an intersection gap. The field of view, 250–320 mm, was adjusted to the size of the breasts to improve spatial resolution at the given matrix.

The dynamic series consisted of 10 individual dynamic images; one was obtained before and nine after the rapid bolus intravenous injection of 0.1 mmol of gadopentetate dimeglumine (Magnevist; Schering, Berlin, Germany) per kilogram of body weight and a 10-mL saline solution flush. The injection and flushing time were set to take 5–7 seconds. Over the whole dynamic series, the system's receiver adjustment remained unchanged.

After the dynamic series, image subtraction was performed to suppress the signal from fat, and enhancing lesions were identified on the subtracted images. To verify the presence of a contrast-enhancing lesion and to exclude subtraction artifacts, we also reidentified the lesions on the nonsubtracted images.

Postprocessing of MR Imaging Data

The enhancement rate was quantified by means of an ROI-based determination of lesion signal intensity before and after the injection of gadopentetate dimeglumine. The relative enhancement (percentage of signal intensity increase) was calculated according to the enhancement formula $(SI_c - SI)/SI \times 100$, where SI and

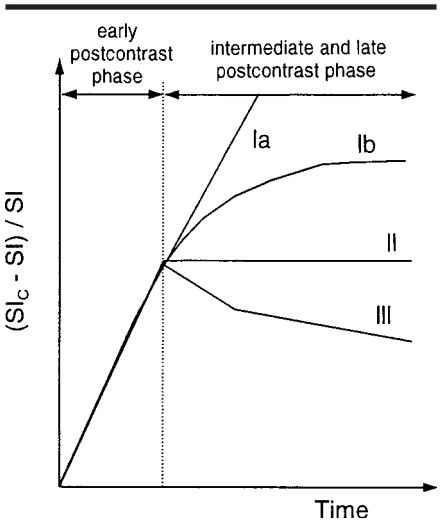

Figure 1. Schematic drawing of the time–signal intensity curve types. Type I corresponds to a straight (*Ia*) or curved (*Ib*) line; enhancement continues over the entire dynamic study. Type II is a plateau curve with a sharp bend after the initial upstroke. Type III is a washout time course ($[SI_c - SI]/SI$).

SI_c are the precontrast and the postcontrast signal intensities, respectively. To assess the early-phase signal intensity increase, we calculated the enhancement for the first postcontrast image. By plotting the lesion signal intensity over time, the time–signal intensity curve was obtained to depict the lesions' enhancement behavior in the early, intermediate, and late postcontrast periods.

Quantitative analysis, plotting, and documentation on hard copy of the signal intensity time courses was performed by a resident (S.K.) who was not involved in reading the film hard copies and who was unaware of the clinical and mammographic findings. Specific care was taken during the placement of the ROI (18–20) so that it was placed selectively in the areas of the most rapid and strongest enhancement (automated ROI definition) (21,22). These areas were identified by means of parametric images that selectively mark and quantify enhancement on the anatomic images. To exclude any partial volume averaging, we adjusted the size of the ROI to the size of the enhancing lesion.

Particular attention was paid to identify any patient motion. Patient motion may lead to faulty time–signal intensity curves if the ROI includes different parts of the lesion or even pixels of the adjacent breast parenchyma from one dynamic image to the other. No attempt was made to trace manually the ROI in a moving lesion between the different dynamic images, because the motion usually does not remain in-plane. In cases of excessive patient motion, the study was not used for diagnosis, and the patient had to come back for a second examination. Of the 230 studies, three had to be repeated owing to excessive patient motion. For data analysis, the lesions were documented together with the corresponding time–signal intensity curves on the film hard copies.

Correlative Imaging Studies and Clinical Information

All patients underwent two-view mammography (Mammomat 3000; Siemens Medical Systems, Erlangen, Germany) with spot compression where appropriate, as well as high-frequency breast US (7.5-MHz probe; model SSA-340A; Toshiba Medical Systems, Neuss, Germany) prior to breast MR imaging. Immediately before the breast MR study, a thorough history was taken of each patient, focusing on recent, prior, or family history of breast diseases. Moreover, all patients were asked to fill out a questionnaire asking for all issues relevant to breast imaging, including menstrual cycle history, hormone intake, prior gynecologic surgery, and prior breast imaging studies. A clinical breast examination was performed, including examination of regional lymph nodes, and the findings were documented on the patient charts. All these data were used to establish the clinical diagnoses in the patients, but they were withheld from the radiologists who were involved in reading the signal intensity time course data.

Data Analysis

The data analysis was designed to assess the diagnostic value of lesion enhancement kinetics (as represented by the time–signal intensity curve) as selectively as possible. Accordingly, two radiologists (C.K.K., P.M.), both trained in reading breast MR imaging studies, were blinded to the clinical, mammographic, and US findings, as well as to patient history; the film hard copies were made anonymous and each was attributed a case number. The ratings by the individual readers were documented together with the case numbers. For reading the curve shape, a postcontrast subtracted image of the lesion was presented with its time–signal intensity curve. The readers were asked to assess independently of each other the lesion's time–signal intensity curve and to classify the curve as steady (type I), plateau (type II), or washout (type III) as shown in Figure 1.

The three curve types differ in their signal intensity time courses in the intermediate and late postcontrast periods. Type I is straight or curved. In type Ia, the straight type, the signal intensity continues to increase over the entire dynamic period; in type Ib, the curved type, the time–signal intensity curve is flattened in the late postcontrast period because of saturation effects. Type II is a plateau in which there is an initial upstroke, after which enhancement is abruptly cut off, and the signal intensity plateaus in the intermediate and late postcontrast periods. Type III is a washout in which there is an initial upstroke, after which enhancement is abruptly cut off, and the signal intensity decreases (washes out) in the intermediate postcontrast period (ie, 2–3 minutes after injection of contrast material).

On the basis of the preliminary experiences triggering this study and from the experiences published in the literature (9,11), the lesions were classified according to the different time–signal intensity curves. A type I time course was rated to be indicative of a benign lesion, type II was rated as suggestive of malignancy, and type III was rated as indicative of a malignant lesion. By using these data, the diagnostic indices—sensitivity, specificity, negative and positive predictive values, and diagnostic accuracy—of the shape of the time–signal intensity curve were determined.

After film hard copy reading, we documented how often the readers provided discordant decisions concerning the time course classification. These cases were then reviewed by both radiologists on a separate occasion, and consensus was obtained for a final time course classification.

The early-phase lesion enhancement rates were quantified as explained, but this information was not made available to the radiologists at the time of time–signal intensity curve reading. Mean enhancement rates of breast cancers, benign solid lesions, and nonproliferative or proliferative fibrocystic changes were calculated.

Because an enhancement rate criterion has been suggested in the dynamic breast MR imaging literature (18), a relative signal intensity increase of more than 60% on the first postcontrast image was considered indicative of breast cancer. This enhancement threshold has been described previously (18) and has been defined with reference to the mean early-phase enhancement rates of breast cancers ±

SD. Thus, lesions were classified according to their early-phase enhancement rates as benign if the relative signal intensity increase was less than or equal to 60%, indeterminate if it was more than 60% and less than or equal to 80%, and malignant if it was more than 80%.

To determine the diagnostic accuracies, we compared lesion classifications on the basis of the enhancement rates and curve types with the lesions' definitive diagnoses.

Statistical Methods

The SPSS software package version 6.13 (SPSS, Chicago, Ill) was used for statistical data analysis. The Student *t* test for independent samples was applied to check for a statistically significant difference between the enhancement rates of benign and malignant lesions. To test the significance of the curve type distribution in benign and malignant lesions, we used the χ^2 test, including directional and symmetric measures as given by the λ and ϕ values. To determine the interreader agreement, we calculated the κ coefficient. For all tests, a *P* value less than .01 was used to indicate significance.

RESULTS

Lesion Diagnoses

Of the 266 contrast-enhancing lesions, 98 were primary breast cancers, and three were malignant tumors other than breast cancer—primary breast lymphoma, malignant cystosarcoma phyllodes, and metastatic seed of an ovarian cancer to the right breast. The primary breast cancers consisted of 58 ductal invasive cancers not otherwise specified, four tubular cancers, three medullar cancers, and one mucinous cancer; 21 lobular invasive cancers; and 11 ductal in situ cancers. Of the 165 benign lesions, 103 were benign solid tumors (adenoma, fibroadenoma), and 62 were fibrocystic changes. The diagnoses were confirmed by means of excisional biopsy or core biopsy for all malignant lesions, 55 of 103 benign solid tumors, and six of 62 fibrocystic changes; these cases were followed up for at least 2 years in 104 lesions (48 of 103 benign solid tumors and 56 of 62 fibrocystic changes).

Early-Phase Enhancement Rate

Enhancement values of benign and malignant lesions differed significantly ($P < .001$); the early postcontrast signal intensity increase was markedly stronger in malignant lesions (Fig 2) than in benign lesions. The mean enhancement rate of malignant lesions was 104% ± 41. The mean enhancement rate of benign lesions was 72% ± 35 (75% ± 36 for solid tumors and 67% ± 31 for fibrocystic changes). The medians for the enhancement rates of malignant lesions, benign solid tumors, and fibrocystic changes were 95%, 70%, and 65%, respectively. Yet because of the broad SD, the ranges of enhancement rates of benign and malignant lesions overlapped considerably (Fig 2, Table 1).

According to the classification of enhancement rates used here, with enhancement less than or equal to 60% for a benign lesion, enhancement of more than 60% and less than or equal to 80% for an indeterminate lesion, and enhancement of more than 80% for a malignant lesion, the following diagnostic indices emerge: sensitivity, 91% (92 of 101); specificity, 37% (61 of 165); positive predictive value, 47% (92 of 196); negative predictive value, 87% (61 of 70); and diagnostic accuracy, 58% (153 of 266).

TABLE 1
Enhancement Rates in Breast Cancers, Benign Solid Tumors, and Fibrocystic Changes

Enhancement	Malignant Lesions (*n* = 101)	Benign Solid Lesions (*n* = 103)	Nonproliferative or Proliferative Fibrocystic Changes (*n* = 62)
Slow	9 (9.0)	35 (34.0)	26 (42)
Intermediate	26 (25.7)	26 (25.2)	21 (34)
Fast	66 (65.3)	42 (40.8)	15 (24)

Note.—Slow enhancement is defined as a signal intensity increase less than or equal to 60% on the first postcontrast image. Intermediate enhancement is defined as a signal intensity increase of more than 60% and less than or equal to 80% on the first postcontrast image. Fast enhancement is defined as a signal intensity increase of more than 80% on the first postcontrast image.
Data in parentheses are percentages.

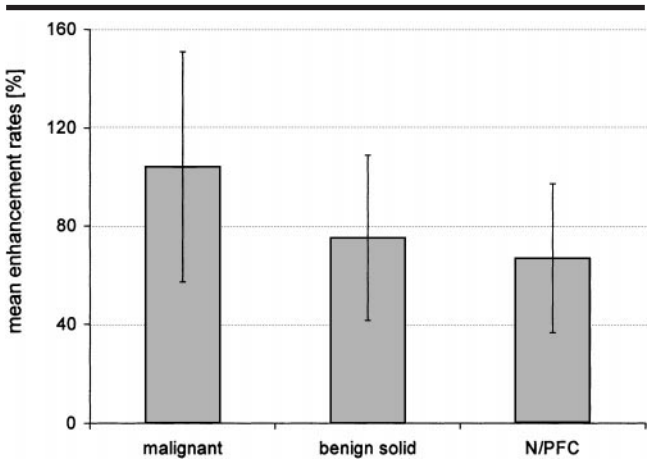

Figure 2. Bar graph shows the mean early-phase enhancement rates in breast cancers, benign solid tumors, and fibrocystic changes (*N/PFC*) ± SD (error bars). Enhancement rates are calculated for the 1st postcontrast minute.

Evaluation of the Shape of the Time–Signal Intensity Curves

The shapes of the time–signal intensity curves of benign and malignant lesions differed significantly; the data are shown in Figure 3.

In benign solid tumors and in fibrocystic changes, the predominant signal intensity time course was type I (ie, a straight or curved time course with steady signal intensity increase). It was found in 83.0% (137 of 165) of benign contrast-enhancing lesions. A type II curve was identified in 11.5% (19 of 165) of cases; a type III curve was obtained in 5.5% (nine of 165) of cases (Fig 3).

In malignant lesions, a type III curve was seen in 57.4% (58 of 101), while a type II curve occurred in 33.6% (34 of

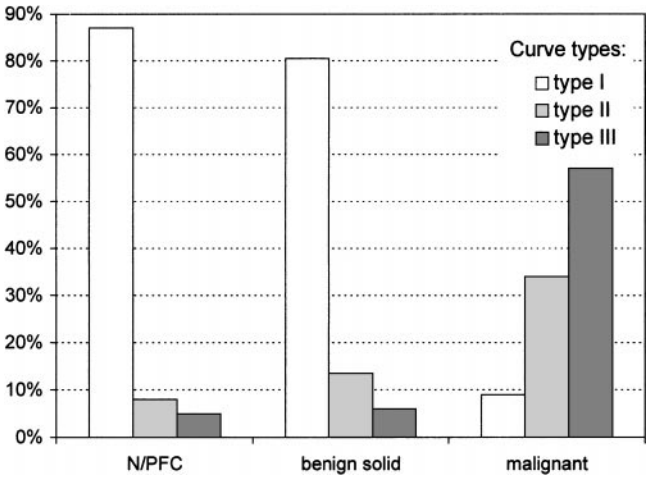

Figure 3. Bar graph shows the distribution of time–signal intensity curve types in malignant lesions, benign solid lesions, and fibrocystic changes (*N/PFC*).

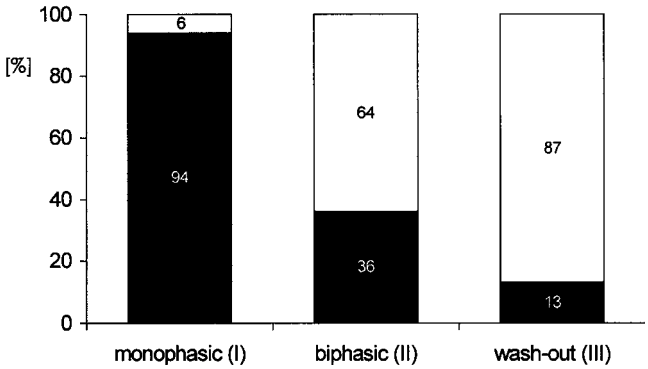

Figure 4. Bar graph shows the prevalence of benign (black bars) and malignant (white bars) lesions for the three different signal intensity time courses.

TABLE 2
Visual Assessment of Curve Types in 266 Lesions: Comparison of Ratings between Reader 1 and Reader 2

Rating Reader 1	Rating Reader 2		
	Type I	Type II	Type III
Type I	139	8	0
Type II	4	42	1
Type III	0	11	61

101). A type I curve was present in 8.9% (nine of 101). The χ^2 test demonstrated a statistically significant difference in the distribution of the curve types in benign and malignant lesions; χ^2 was 139.6, λ was 0.511, and ϕ was 0.734 ($P < .001$).

If types II and III (ie, plateau and washout time courses) are used as criteria to diagnose breast cancer, and a type I time course (ie, steadily increasing signal intensity) is considered suggestive of a benign lesion, the following diagnostic indices for the shape of the time–signal intensity curve criterion emerged: sensitivity, 91% (92 of 101); specificity, 83% (137 of 165); positive predictive value, 77% (92 of 120); negative predictive value, 94% (137 of 146); and diagnostic accuracy, 86% (229 of 266). The likelihood of breast cancer associated with a type I, II, or III time course was 6% (nine of 146), 64% (34 of 53), and 87% (58 of 67), respectively (Fig 4).

Interreader Variability of Signal Intensity Time Course Classification

In 242 (91%) of 266 cases, the two readers came to concordant results in signal intensity time course classification. In the 24 cases with discordant rating, the classification differed between types I and II or between types II and III (Table 2). In none of the cases did the classification differ between types I and III. The κ coefficient was 0.849, indicating significant interreader agreement ($P < .001$).

DISCUSSION

Breast MR imaging is increasingly used in addition to conventional breast imaging modalities such as mammography and breast US. It is used to help diagnose primary and recurrent breast cancer in cases in which mammography and breast US are inconclusive or yield discrepant results (4,7,9). Moreover, breast MR imaging may improve the local staging of breast cancer by revealing multifocal tumor growth in patients scheduled for conservative breast surgery (1). While the excellent sensitivity of breast MR imaging proves particularly advantageous for its application in the preoperative patient, its limited specificity continues to be problematic, particularly in patients referred for clarification of a conventionally inconclusive finding (23).

In principle, two different approaches have been pursued to improve the technique's specificity: Single-breast imaging protocols with high spatial resolution aim at a meticulous analysis of the lesion's structure and internal architecture to distinguish benign from malignant lesions (2,3,5). On the other hand, lesion differential diagnosis in dynamic protocols is based on the assumption that benign and malignant lesions are distinguishable owing to their different enhancement kinetics (8,9,11,15,17).

The lesion enhancement rate in the early postcontrast period (also known as ''enhancement velocity'' or ''slope of enhancement'') serves as a differential diagnostic criterion, with malignant lesions exhibiting stronger and faster enhancement than benign changes do. Yet, growing clinical experience revealed that a considerable number of benign proliferative changes and benign solid tumors demonstrate enhancement rates comparable to those of malignant lesions, thus again reducing the technique's specificity (7,24). Accordingly, some authors (9,11, 12,24–26) suggest assessing the lesions' signal intensity behavior in the intermediate and late postcontrast periods as depicted by means of the lesion's time–signal intensity-curve. However, diverging results were recently published concerning the diagnostic value of the signal intensity time course data (2,27).

Our results indicate that the enhancement kinetics, as represented by the time–signal intensity curves, differ significantly for benign and malignant enhancing lesions and may therefore be used as an aid in differential diagnosis (Figs 5,6). In breast cancers, plateau or washout time courses (type II or III) prevail. In contrast, benign enhancing lesions exhibit steadily progressive signal intensity time courses (type I); both benign tumors and fibrocystic changes share these enhancement kinetics.

According to the data in our study population, a positive washout phenomenon (type III) is associated with a likelihood of breast cancer of 87% (Fig 4), whereas a progressive signal intensity increase (type I) is associated with a likelihood of breast cancer of only 6%, irrespec-

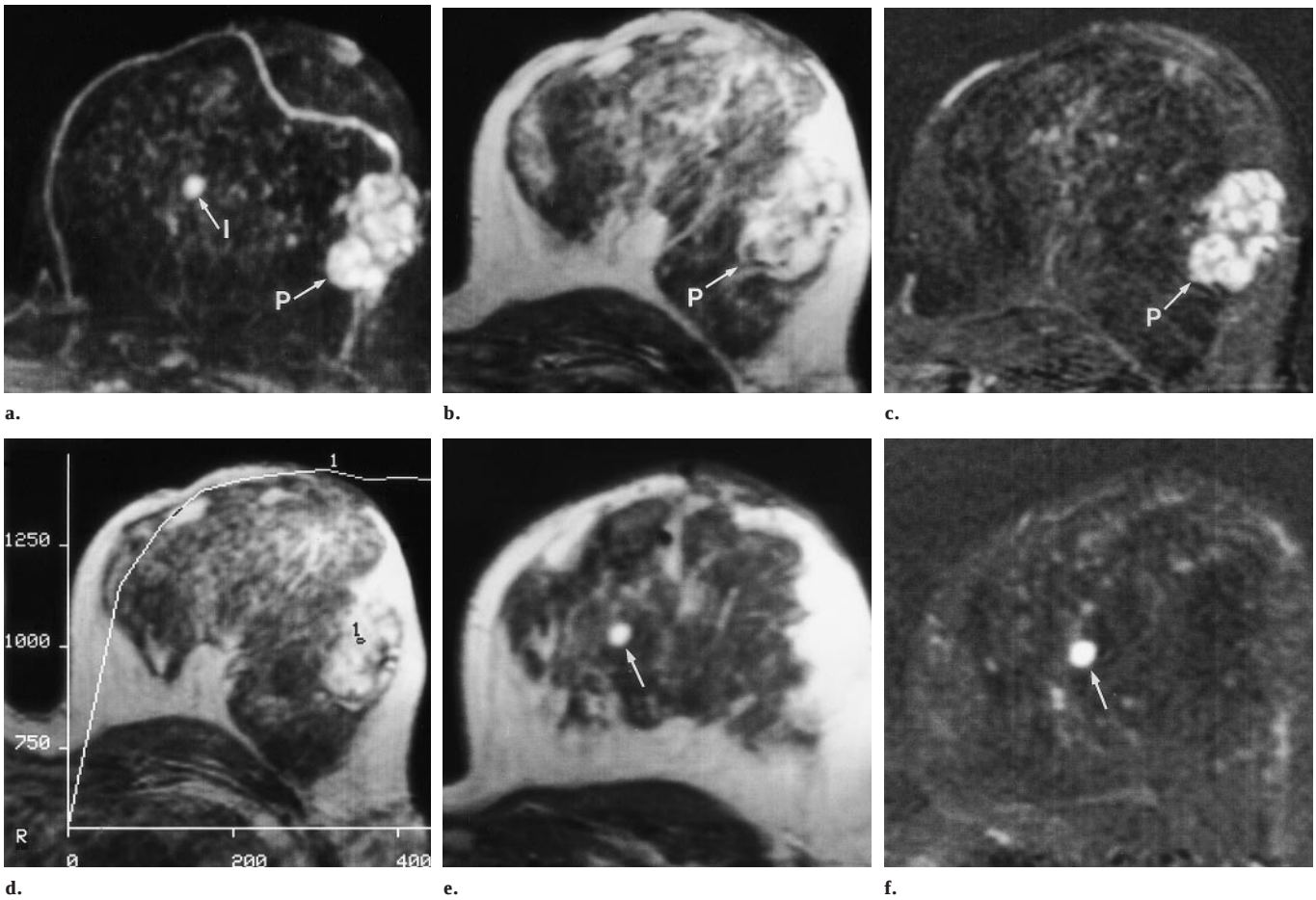

Figure 5. Breast MR images acquired in a 55-year-old patient with a palpable mass in the left upper outer quadrant. The mass had been rated as probably benign on the basis of mammographic and US findings. **(a)** Axial maximum intensity projection MR image from an early postcontrast subtracted data set of the diagnostic breast MR imaging study (220/4.5; flip angle, 80°). The maximum intensity projection image depicts two lesions (arrows): the expected palpable mass (*P*) and a nonpalpable, incidental lesion (*I*) in the left breast. **(b)** Early postcontrast and **(c)** subtracted MR images from the dynamic series (220/4.5; flip angle, 80°) show the palpable mass (*P*). **(d)** Time–signal intensity curve of the palpable mass shows a type I time course. The x axis shows the dynamic imaging beginning time in seconds, and the y axis shows the intensity in arbitrary units. The palpable mass visible in **b–d** exhibits a suggestively strong early-phase enhancement, but it is well circumscribed, has a lobulated appearance, and reveals internal septations, which are all findings consistent with fibroadenoma. **d** further supports the diagnosis of a fibroadenoma. The signal intensity time course corresponds to a type Ib curve. **(e)** Early postcontrast and **(f)** subtracted MR images from the dynamic series (220/4.5; flip angle, 80°) obtained several sections cephalad of the palpable mass in **b–d** show the incidental lesion (arrow). **(g)** Time–signal intensity curve of the incidental lesion shows a type III time course. The x axis shows the dynamic imaging beginning time in seconds, and the y axis shows the intensity in arbitrary units. The small, incidental, nonpalpable lesion visible in **e–g** shows the same rapid enhancement as the lesion visible in **b–d**. Also, it is well circumscribed and enhances homogeneously. However, it has a type III (washout) curve, which prompted the prospective diagnosis of an occult breast cancer, together with a fibroadenoma, in the same breast. Because the incidental lesion visible in **e–g** remained invisible at mammography (including spot compression) and at directed high-frequency breast US, excisional biopsy was performed after MR-guided stereotactic needle localization. Histologic confirmation of a 6-mm ductal invasive breast cancer pT1bN0M0 was obtained for the incidental lesion visible in **e–g**, and confirmation of a myxoid fibroadenoma was obtained for the palpable lesion visible in **b–d**.

tive of other imaging findings that may and should be used in addition. A plateau signal intensity time course (type II) is seen both in malignant and benign lesions but with a distribution of three to two. Therefore, a type II time course should be used to support the suspicion of breast cancer.

There are some possible sources of bias in this study, owing to the specific inclusion criteria and the way the curve shape reading was performed.

Concerning the histologic distribution of lesions in our study group, the rate of fibrocystic changes is lower and the rate of malignant tumors is higher than expected. This is probably in part because preoperative staging to rule out multifocal breast cancer is one of the most important indications for breast MR imaging in

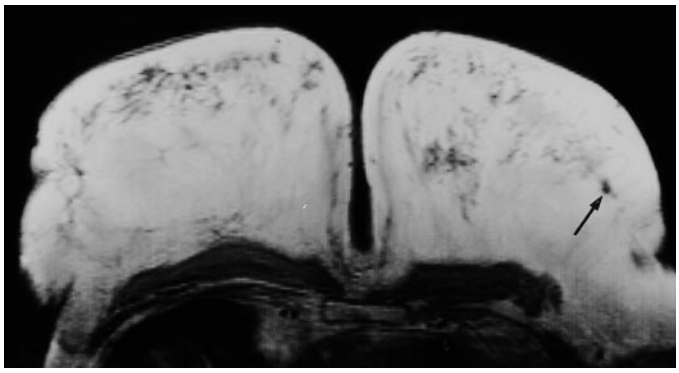

a.

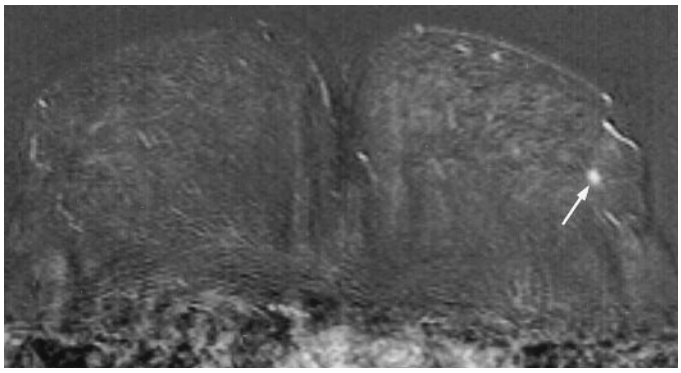

b.

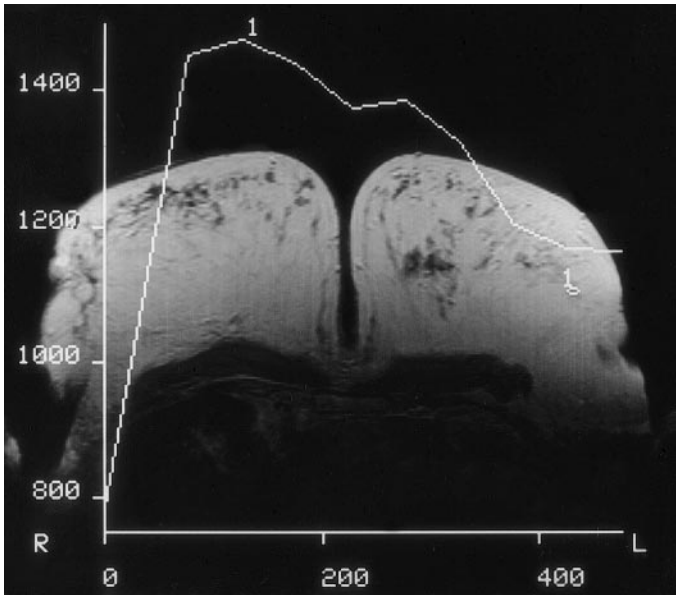

c.

Figure 6. MR images acquired in a 55-year-old patient who underwent breast MR imaging for routine follow-up after breast-conservation therapy and radiation therapy of her right breast 2 years previously. **(a)** Precontrast and **(b)** early postcontrast subtracted MR images (220/4.5; flip angle, 80°) from the dynamic breast study reveal a small lesion (arrow) with intermediate enhancement in the upper outer quadrant of the contralateral (left) breast. There is no enhancement in the scar tissue from the tumor removal on the right side. **(c)** Time–signal intensity curve of the lesion in the left breast shows that the early-phase enhancement rate is 75%. The x axis shows the dynamic imaging beginning time in seconds, and the y axis shows the intensity in arbitrary units. There is a washout of signal intensity in the intermediate postcontrast period, corresponding to a type III curve. Excisional biopsy findings confirmed the presence of a 6-mm invasive tubular breast cancer. There was no axillary lymph node involvement.

our patients. More important, the selection criteria cause a bias in that only lesions with suggestive enhancement have been considered. The majority of fibrocystic changes did not fit into this category but had a slowly progressive, nonsuggestive enhancement. Accordingly, all breast cancers that were diagnosed during the study period, but by far not all of the benign fibrocystic parenchymal changes, have been included. Also, the low fraction of ductal carcinoma in situ among the malignant lesions is possibly owing to the inclusion criteria but also may be because patients in whom ductal carcinoma in situ is suspected on the basis of mammographic or US findings do not undergo breast MR imaging because of its questionable sensitivity for ductal carcinoma in situ.

The specific inclusion criteria may introduce a bias toward invasive malignant lesions. However, without these inclusion prerequisites, negative breast MR imaging studies with no or slowly progressive enhancement (ie, with type I time course) would have been included. This would lead to an artificial increase in specificity levels. Accordingly, the bias introduced by the inclusion criteria puts breast MR imaging at a disadvantage; it is much more demanding to classify as benign a breast MR imaging study with an enhancing lesion rather than a completely negative study without enhancement. Moreover, the inclusion criteria match with the specific objective of this study—the investigation of a diagnostic criterion to aid in the differential diagnosis of enhancing lesions. Without enhancement, there is no breast MR imaging differential diagnosis necessary or possible. With the inclusion criteria used here, we were able to give an authentic and accurate evaluation of the differential diagnostic potency of the criteria under investigation.

Among the malignant lesions, the high rate of lobular cancers in this study group is striking. This high fraction is probably attributable to the fact that, in the Department of Radiology, University of Bonn, Germany, another major reason to perform breast MR imaging is clarification of an indeterminate mammographic finding. In particular, lobular cancers may exhibit nonspecific findings on mammograms (no microcalcifications) such that breast MR imaging is desired (or even required) for clarification. Accordingly, because of this particular patient preselection bias, the data may be skewed toward a higher-than-expected prevalence of lobular cancers.

Every attempt was made to deprive the time course readers of clinical, mammographic, and US information to ensure a blinded analysis. However, as dictated by the software used for time course analysis, the time–signal intensity curves are presented together with a postcontrast subtracted image of the same lesions. This provides some morphologic information that might introduce a bias for the experienced breast MR imaging reader.

It is important to note that the kinetic time course data presented here stem from a dynamic protocol that covers both entire breasts. In contrast with fast dynamic single-section techniques that merely aim at the further differential

diagnosis of lesions that are previously known (6), the whole-breast dynamic protocol is suitable for all current clinical applications of breast MR imaging, particularly preoperative local staging.

The diverging results published in the literature concerning the value of time course data in dynamic whole-breast MR imaging might in part be owing to the differing imaging techniques that have been used in the studies (27). Temporal resolution seems crucial to detect washout phenomena in which the peak enhancement occurs within the first 2 postcontrast minutes. Imaging protocols with lower temporal resolution might miss a washout phenomenon if the first postcontrast image is obtained only after the peak enhancement (ie, during the descending part of the time–signal intensity curve). False-positive washout phenomena (ie, washout phenomena in benign lesions) have been reported to occur more often with three-dimensional gradient-echo imaging techniques, which is one reason why a two-dimensional technique is used in the Department of Radiology, University of Bonn (28). Also, the three curve types are distinguishable only as long as the data points are not interpolated, because this would smooth out any sharp bends or washout effects.

The specificity level in this study is lower than that in a previously published study (9) in which a comparable imaging technique was used. A reason for this might be the specific inclusion criteria used in this study that aimed at the differential diagnosis of enhancing lesions.

The biologic or pathophysiologic correlate of the differing time courses remains speculative, yet the detection of a washout phenomenon suggests the presence of an increased vessel density and arteriovenous anastomoses with rapid outflow and thus fading of the contrast material (29–31). The changes of resistive index found in Doppler US studies of breast cancers have been attributed to the presence of arteriovenous anastomoses, and histopathologic studies have confirmed this assumption (32–34). So far, we do not have histologic data to clarify the pathophysiologic nature of the washout phenomenon, but a study by us focusing on this issue is underway.

Particularly in premenopausal patients (24,26), the washout effect may have an important effect on the detectability of breast cancers. In these patients, the washout-induced signal intensity loss in breast cancers may be associated with a strong and rapid increase in signal intensity in the adjacent breast parenchyma (Fig 7). Accordingly, the lesion-to-parenchyma contrast diminishes in the intermediate and late postcontrast periods, which may substantially reduce the visibility of breast cancers. Therefore, in these patients, an adequate temporal resolution may be not only helpful for lesion characterization but also required to better detect malignant lesions.

The visual classification of the shape of the signal intensity time courses was reproducible between readers. With a interreader agreement rate of 91%, and a κ coefficient of 0.849, the time course assessment qualified as a stable diagnostic criterion reproducible enough to compare favorably with other criteria in the field of diagnostic imaging in general or with conventional or MR breast imaging in particular (35–39).

When compared with the diagnostic information provided by the enhancement rate criterion, that provided by the signal intensity time courses is substantially more specific in identifying breast cancer, with a specificity of 83% versus a specificity of 37% for the enhancement rate criterion. Most important, this gain in specificity is achieved without loss of sensitivity, which was 91% for both criteria.

In terms of the diagnostic value of early-phase enhancement rates, the study data demonstrate that the concept of enhancement thresholds that was proposed for differential diagnosis in dynamic breast MR imaging (9) is not only problematic in leading to false-positive diagnoses in lesions with rapid enhancement (two-thirds of the benign lesions had suprathreshold enhancement rates) but also prone to cause false-negative decisions (Fig 6). The results add further evidence to the concept of a synoptic approach to the differential diagnosis of enhancing breast lesions, an approach that does not focus on enhancement kinetics alone but that includes other diagnostic criteria, particularly morphologic data, to improve both sensitivity and specificity.

This study was undertaken to investigate whether the insight into lesions' enhancement kinetics, as provided by a bilateral whole-breast technique, does provide diagnostically useful information. The results suggest that also with the limited temporal resolution achievable in this setting, the signal intensity time course data are helpful for lesion differential diagnosis. In the future, another important issue will be to decide whether in general high temporal or high spatial resolution should have priority in breast MR imaging protocols; further studies with intraindividual comparison are required to answer this question. With the technical equipment currently available, all protocols will more or less represent a compromise on these diverging demands; however, the results of this study support the concept of dynamic image acquisition in future breast MR imaging protocols.

In conclusion, our results indicate that time–signal intensity curves obtained from dynamic MR images of enhancing breast lesions provide diagnostically useful information. The evaluation of time–signal intensity curves seems suitable to assist in lesion differential diagnosis, thus contributing to an improved overall specificity of dynamic breast MR imaging. The differential diagnostic potency of the signal intensity time course is superior to the established diagnostic criterion of dynamic breast MR imaging (ie, the enhancement rate). Although both are related to lesion enhancement, the criteria of the enhancement rate and the shape of the time–signal intensity curve appear to represent independent features. Visual assessment of the shape of the time–signal intensity curve is reproducible enough to allow a reliable classification.

In practice, at the Department of Radiology, University of Bonn, evaluation of lesion time course kinetics has already had considerable effect on the management of lesions in breast MR imaging. It should be well understood that the analysis of lesion enhancement kinetics should not be used as a stand-alone diagnostic criterion but that it should be integrated into the process of lesion differential diagnosis. The following principles must be kept in mind when dealing with time courses.

First, the time–signal intensity curve analysis seems most useful in the differential diagnosis of focal lesions with rapid enhancement. In malignant lesions with slow enhancement, the underlying poor angiogenic activity may also prevent a washout or plateau time course. Accordingly, particularly lobular or scirrhous ductal invasive cancers (and possibly also ductal carcinoma in situ) with slow or gradual enhancement may exhibit type I time courses. However, in these lesions, morphology is almost always suggestive in the first place, such that a time course analysis is not indicated (described later).

Second, a washout phenomenon is a very specific, albeit not very sensitive, indicator of malignancy; 87% of lesions with washout are malignant, but washout is seen in only 57% of malignancies.

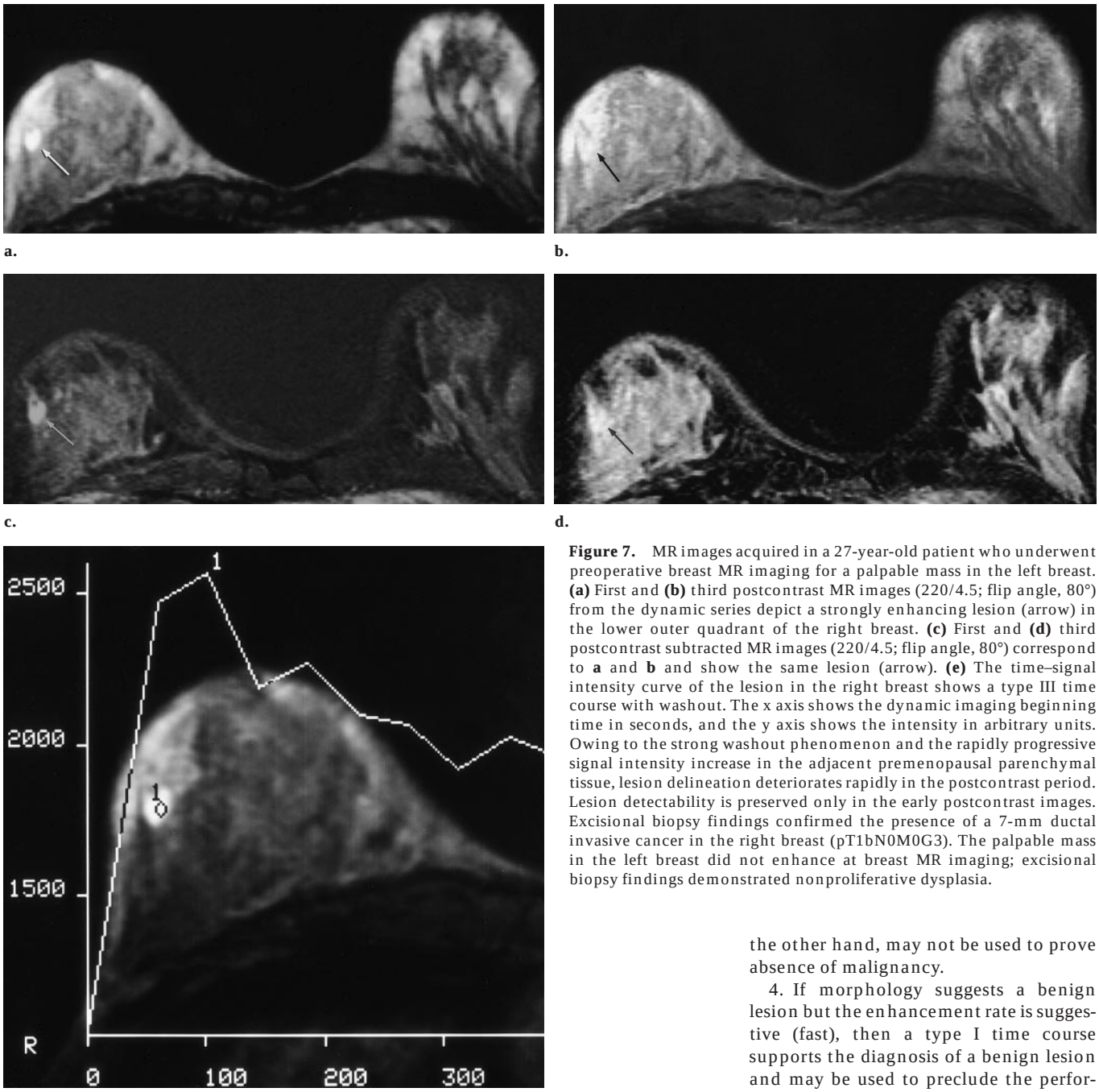

Figure 7. MR images acquired in a 27-year-old patient who underwent preoperative breast MR imaging for a palpable mass in the left breast. **(a)** First and **(b)** third postcontrast MR images (220/4.5; flip angle, 80°) from the dynamic series depict a strongly enhancing lesion (arrow) in the lower outer quadrant of the right breast. **(c)** First and **(d)** third postcontrast subtracted MR images (220/4.5; flip angle, 80°) correspond to **a** and **b** and show the same lesion (arrow). **(e)** The time–signal intensity curve of the lesion in the right breast shows a type III time course with washout. The x axis shows the dynamic imaging beginning time in seconds, and the y axis shows the intensity in arbitrary units. Owing to the strong washout phenomenon and the rapidly progressive signal intensity increase in the adjacent premenopausal parenchymal tissue, lesion delineation deteriorates rapidly in the postcontrast period. Lesion detectability is preserved only in the early postcontrast images. Excisional biopsy findings confirmed the presence of a 7-mm ductal invasive cancer in the right breast (pT1bN0M0G3). The palpable mass in the left breast did not enhance at breast MR imaging; excisional biopsy findings demonstrated nonproliferative dysplasia.

Thus, concerning the integration of our study results into the process of differential diagnosis of enhancing breast MR lesions, the following guidelines have emerged:

1. Analysis of time course kinetics is done after the evaluation of the lesions' morphology in postcontrast images. If morphology is clearly suggestive, we do not evaluate kinetics for reasons explained earlier. If morphology is indeterminate or suggests a benign lesion, we recommend performing a time–signal intensity curve analysis.

2. If morphology suggests a benign or indeterminate lesion, but a washout time course is detected, biopsy must be performed on the lesion. A washout constitutes an absolute indication to perform biopsy on a lesion, irrespective of other MR criteria (particularly morphology and enhancement rate) or conventional imaging findings (Figs 5–7).

3. Lack of a washout phenomenon, on the other hand, may not be used to prove absence of malignancy.

4. If morphology suggests a benign lesion but the enhancement rate is suggestive (fast), then a type I time course supports the diagnosis of a benign lesion and may be used to preclude the performance of biopsy.

5. If, in an incidental lesion, morphology is indeterminate, and possibly even enhancement rates are suggestive, a type I time course can help preclude the performance of biopsy as long as no other (particularly mammographic) findings raise suspicion and provided a close follow-up is possible. This is an important means to reduce false-positive biopsy findings of incidental lesions in young premenopausal patients (24).

6. If morphology suggests a malignant lesion, a time course analysis is not indicated, because it has no effect on further

lesion management. The time–signal intensity curve analysis in these cases can be used only to confirm the presence of breast cancer. Even if slow and gradual enhancement rates indicate a benign lesion, a type I time–signal intensity curve may not be used to preclude the performance of biopsy, because the lesions may represent lobular or scirrhous ductal cancer.

References

1. Orel SG, Schnall MD, Powell CM, et al. Staging of suspected breast cancer: effect of MR imaging and MR-guided biopsy. Radiology 1995; 196:115–122.
2. Orel SG, Schnall MD, LiVolsi VA, Troupin RH. Suspicious breast lesions: MR imaging with radiologic-pathologic correlation. Radiology 1994; 190:485–493.
3. Harms SE, Flamig DP, Hesley KL, et al. MR imaging of the breast with rotating delivery of excitation off resonance: clinical experience with pathologic correlation. Radiology 1993; 187:493–501.
4. Harms SE, Flamig DP. MR imaging of the breast. JMRI 1993; 3:277–283.
5. Nunes LW, Schnall MD, Orel SG, et al. Breast MR imaging: interpretation model. Radiology 1997; 202:833–841.
6. Boetes C, Barentsz JO, Mus RD, et al. MR characterization of suspicious breast lesions with a gadolinium-enhanced TurboFLASH subtraction technique. Radiology 1994; 193:777–781.
7. Heywang SH. Contrast enhanced magnetic resonance imaging of the breast. Invest Radiol 1994; 29:94–104.
8. Heywang SH, Wolf A, Pruss E, Hilbertz T, Eiermann W, Permanetter W. MR imaging of the breast with Gd-DTPA: use and limitations. Radiology 1989; 171:95–103.
9. Kaiser WA, Zeitler E. MR imaging of the breast: fast imaging sequences with and without Gd-DTPA—preliminary observations. Radiology 1989; 170:681–686.
10. Perman WH, Heiberg EM, Grunz J, Herrmann VM, Janney CG. A fast 3D-imaging technique for performing dynamic Gd-enhanced MRI of breast lesions. Magn Reson Imaging 1994; 12:545–551.
11. Fischer U, von Heyden D, Vosshenrich R, Vieweg I, Grabbe E. Signalverhalten maligner und benigner läsionen in der dynamischen 2D-MRT der mamma. ROFO 1993; 158:287-292
12. Heiberg EV, Perman WH, Herrmann VM, Janney CG. Dynamic sequential 3D gadolinium-enhanced MRI of the whole breast. Magn Reson Imaging 1996; 14:337–348.
13. Gribbestad IS, Nilsen G, Fjosne H, et al. Contrast-enhanced magnetic resonance imaging of the breast. Acta Oncol 1992; 31:833–842.
14. Flickinger FW, Allison JD, Sherry RM, Wright JC. Differentiation of benign from malignant breast masses by time-intensity evaluation of contrast enhanced MRI. Magn Reson Imaging 1993; 11:617–620.
15. Gilles R, Guinebretiere JM, Lucidarme O, et al. Nonpalpable breast tumors: diagnosis with contrast-enhanced subtraction dynamic MR imaging. Radiology 1994; 191:625–631.
16. Hulka CA, Smith BL, Sgroi DC, et al. Benign and malignant breast lesions: differentiation with echo-planar MR imaging. Radiology 1995; 197:33–38.
17. Kelcz F, Santyr GE, Cron GO, Mongin SJ. Application of a quantitative model to differentiate benign from malignant breast lesions detected by dynamic, gadolinium-enhanced MRI. JMRI 1996; 6:743–752.
18. Gribbestad IS, Nilsen G, Fjosne HE, Kvinnsland S, Haugen OA, Rinck PA. Comparative signal intensity measurements in dynamic gadolinium-enhanced MR mammography. JMRI 1994; 4:477–480.
19. Revel D, Brasch RC, Paajanen H, et al. Gd-DTPA contrast enhancement and tissue differentiation in MR imaging of experimental breast carcinoma. Radiology 1986; 158:319–323.
20. Mussurakis S, Buckley DL, Coady AM, Turnbull LW, Horsman A. Observer variability in the interpretation of contrast enhanced MRI of the breast. Br J Radiol 1996; 69:1009–1016.
21. Mussurakis S, Buckley DL, Horsman A. Dynamic MRI of invasive breast cancer: assessment of three region-of-interest analysis methods. J Comput Assist Tomogr 1997; 21:431–438.
22. Kuhl C, Bieling H, Lutterbey G, Sommer T, Schild HH. Standardisierung und beschleunigung dynamischer MR-mammographien durch parameterbilder und automatische ROI-definition. ROFO 1996; 164:475–482.
23. Piccoli CW. The specificity of contrast-enhanced breast MR imaging. Magn Reson Imaging Clin N Am 1994; 2:557–571
24. Kuhl CK, Kreft BP, Bieling HB, et al. Dynamic breast MRI in premenopausal healthy volunteers: normal values of contrast enhancement and cycle phase dependency. Radiology 1997; 203:1–9.
25. Stack JP, Redmond OM, Codd MB, Dervan PA, Ennis JT. Breast disease: tissue characterization with Gd-DTPA enhancement profiles. Radiology 1990; 17:491–494.
26. Müller-Schimpfle M, Ohmenhauser K, Sand J, Stoll P, Claussen CD. Dynamic 3D-MR mammography: is there a benefit of sophisticated evaluation of enhancement curves for clinical routine? JMRI 1997; 7:236–240.
27. Fobben ES, Rubin CZ, Kalisher L, Dembner AG, Seltzer MH, Santoro EJ. Breast MR imaging with commercially available techniques: radiologic-pathologic correlation. Radiology 1995; 196:143–152.
28. Kuhl CK, Mielcarek P, Schild HH. Sensitivity of 2D and 3D GRE sequences in dynamic breast MR imaging: systematic controlled study with intraindividual comparison (abstr). Radiology 1996; 201(P):130.
29. Frouge C, Guinebretiere JM, Contesso G, Di Paola R, Blery M. Correlation between contrast enhancement in dynamic magnetic resonance imaging of the breast and tumor angiogenesis. Invest Radiol 1994; 29:1043–1049.
30. Gilles R, Zafrani B, Guinebretiere JM, et al. Ductal carcinoma in situ: MR imaging-histopathologic correlation. Radiology 1995; 196:415–419.
31. Buadu LD, Murakami J, Murayama S, et al. Breast lesions: correlation of contrast medium enhancement patterns on MR images with histopathologic findings and tumor angiogenesis. Radiology 1996; 200: 639–649.
32. Rubin JM, Carson PL, Zlotecki RA, Ensminger WD. Visualization of tumor vascularity in a rabbit VX2 carcinoma by Doppler flow mapping. J Ultrasound Med 1987; 6:113–120.
33. Lee WJ, Chu JS, Huang CS, Chang MF, Chang KJ, Chen KM. Breast cancer vascularity: color Doppler sonography and histopathology study. Breast Cancer Res Treat 1996; 37:291–298.
34. Kedar RP, Cosgrove D, McCready VR, Bamber JC, Carter ER. Microbubble contrast agent for color Doppler US: effect on breast masses—work in progress. Radiology 1996; 198:679–686.
35. Baker JA, Kornguth PJ, Floyd CE Jr. Breast imaging reporting and data system standardized mammography lexicon: observer variability in lesion description. AJR 1996; 166:773–778.
36. Beam CA, Layde PM, Sullivan DC. Variability in the interpretation of screening mammograms by US radiologists: findings from a national sample. Arch Intern Med 1996; 156:209–213.
37. Elmore JG, Wells CK, Lee CH, Howard DH, Feinstein AR. Variability in radiologists' interpretations of mammograms. N Engl J Med 1994; 331:1493–1499.
38. Baines CJ, McFarlane DV, Miller AB. The role of the reference radiologist: estimates of inter-observer agreement and potential delay in cancer detection in the national breast screening study. Invest Radiol 1990; 25:971–976.
39. Tudor GR, Finlay D, Taub N. An assessment of inter-observer agreement and accuracy when reporting plain radiographs. Clin Radiol 1997; 52:235–238.